Applicability of Tropical Rainfall Measuring Mission to predict floods on the Bagmati River

Rishi Ram Sharma[1,2], Lal Samarkoon[3], Manzul Hazarika[3] and Tanka Prasad Kafle[3]

[2] *Department of Hydrology and Meteorology, P.O. Box 406, Kathmandu*

[3] *Geoinformatics Centre AIT, Bangkok*

ABSTRACT

In this paper rainfall fields of TRMM 3B42RT were assessed with available point observation data obtained from rain gauges and Automatic Weather Stations (AWS). Rainfall comparison was done on grid basis. It was found that when the number of rainfall stations increased, the discrepancy between the TRMM rainfall and grid average of the observed rainfall decreased, implying that TRMM rainfall was closely associated with the average rainfall falling under the grid domain. It was also inferred that TRMM slightly overestimated the rainfall in dry region (mountain shadow) and underestimated the rain in wetest region during the peak monsoon season. TRMM well captured the diurnal variability as compared to AWS data with two maxima. The TRMM data were then used to predict the daily average discharge of Bagmati River. Regression technique was adopted to predict the daily average discharge at *Pandhera Dovan* gauging site. The model predicted the daily peak discharge very well whereas the erratic fluctuations were obtained during the periods of low flows.

Keywords: TRMM 3B42RT, regression, rainfall-runoff modeling, flood forecasting, Bagmati River

1. INTRODUCTION

The actual amount of rainfall falling under a watershed is the most critical part in rainfall-runoff modeling. Rain-gauges provide point observation, whereas weather radars are capable to measure areal coverage. Both the point and areal measurement have advantages and disadvantages. Rain-gauges are cheaper and simpler in terms of installations, economics and technology. The main concerns are the networks for areal representation. Usually for satellite rainfall validation program dense gauge networks, for example 2 km x 2 km, are used (Sorooshian et al. 2002). Such dense network is difficult for the mountainous country like Nepal. In Nepal, rainfall stations are mostly concentrated in the urban and accessible areas with large void in high mountain regions.

In contrast to point observation, ground radars are highly technical and costly rainfall measuring techniques. They have the capability to provide 3D profile of rainfall, which is useful to understand the complex rainfall process and its interaction with other meteorological fields but they cover limited geographical areas mostly in developed countries.

Various satellite based rainfall products are available from near real-time to monthly average covering different geographical areas with varying grid sizes. (Brown, 2006; Delgado et al. 2006; Xie and Arkin, 1996; Petty, 1995; Gorenburg et al. 2001; Todd et al. 2001; Boi et al. 2004). Different techniques and data are utilized to derive the rainfall estimation. Some approaches such as microwave and Radar techniques are more direct whereas other, visible and infrared techniques, utilized some indirect approach of satellite rainfall estimation (Kidder and Haar, 1995; Levizzani and Amorati, 2002).

One of the satellites devoted to rainfall estimation is Tropical Rainfall Measuring Mission (TRMM).

[1] Corresponding Author (Email: rishisharm@yahoo.com)

It is a joint U.S.-Japan satellite mission to monitor tropical and subtropical precipitation. The TRMM orbit is circular, non-sun-synchronous, at an altitude of 350 km and an inclination of 35 degrees to the equatorial plane. This orbit provides extensive coverage in the tropics and allows each location to be covered at a different local time each day. This kind of sampling enables the analysis of the diurnal cycle of precipitation (Sorooshian et al. 2002).

Various data products are available from the combination of TRMM and other satellites. The combined instrument rain calibration algorithm, 3B42RT (where 3 = processing level, B = level type, 4 = sensor (TRMM and other sources), 2 = algorithm number, RT = Near Real Time), uses optimal combination of visual and infrared, microwave and RADAR. The output of the product is rainfall fields of 0.25° x 0.25° grid with 3 hours temporal resolution and time lag of 6 hours or more (Itou and Kera, 2006).

The study area, the Bagmati River basin, is situated in central Nepal and covers an area of about 3750 sq km. The river originates from Shivapuri Mountain, altitude 2700 m, a northern bound of Kathmandu valley. It is not a perpetual snow fed river. It extends between 26° 42' to 27° 50' North latitude and 85° 02' to 85° 58' East longitude. The Bagmati River and its tributaries mainly exhibit dendrite drainage pattern. Rainfall occurs due to the southeast monsoon which lasts between the months of June to September. The humid air stream blowing from the Bay of Bengal is forced to rise when it meets the Himalaya. As a result, heavy rainfall occurs on some sections of the southern Himalayan slopes. In the lee-ward side of the mountain ranges, rainfall is reduced due to rain shadow effects. More than 80% of the annual rainfall occurs during the months of June to September. In the winter, rainfall is caused by the weather system originating in the Mediterranean region, called westerly disturbances. The rains in their dying stages reach Nepal and cause significant precipitation in western as well as other parts of the country (Bagmati Report, 2005). Bagmati River is one of the most heavily populated flood prone river basin of Nepal. Extreme flooding events in 1993 was responsible for killing 1029 people, affecting 400,000 people, damaging 25,000 houses, destroying 40,000 ha of agriculture land (Bagmati Report, 2005).

In this paper near real-time TRMM 3B42RT data are used to predict the discharge of Bagmati River at *Pandhera Dovan* gauging site. The main objective of the research was to assess 3-hourly rainfall data of TRMM and use this data to predict floods in the Bagmati River. Ultimate goal of the research is to develop a flood forecasting and early warning mechanism using satellite based rainfall.

2. DATA AND METHODS

Rainfall data of 251 stations and 2 Automatic Weather Station (AWS) data of the year 2004, and daily average discharge of Bagmati River from the year 1979 to 2005 were obtained from the Department of Hydrology and Meteorology of Nepal. The hydrograph of monthly maximum, mean and minimum for June to September, year 1979 to 2005, measured at *Pandhera Dovan* of Bagmati River is shown in Figure 1. *Pandhera Dovan* gauging site is located in such a strategic location that down stream of the gauging site is flood plain and up stream is valley and mountainous. Out of the total area covered by the basin, the flood plain alone is about 20 % of the basin area.

The figure shows that there are 25, 12, 7, and 3 events with monthly maximum more than 2000, 3000, 4000, and 5000 $m^3 s^{-1}$ respectively. The figure also shows that monthly maximum in 1993 had crossed over 7500 $m^3 s^{-1}$. But the instantaneous value of the discharge was 16,000 $m^3 s^{-1}$ which was devastating flood of more than 100 years return period (DHM, 2007).

Three-hourly TRMM 3B42RT rainfall data covering the Bagmati River basin was downloaded from NASA web site (http://trmm.gsfc.nasa.gov/). The

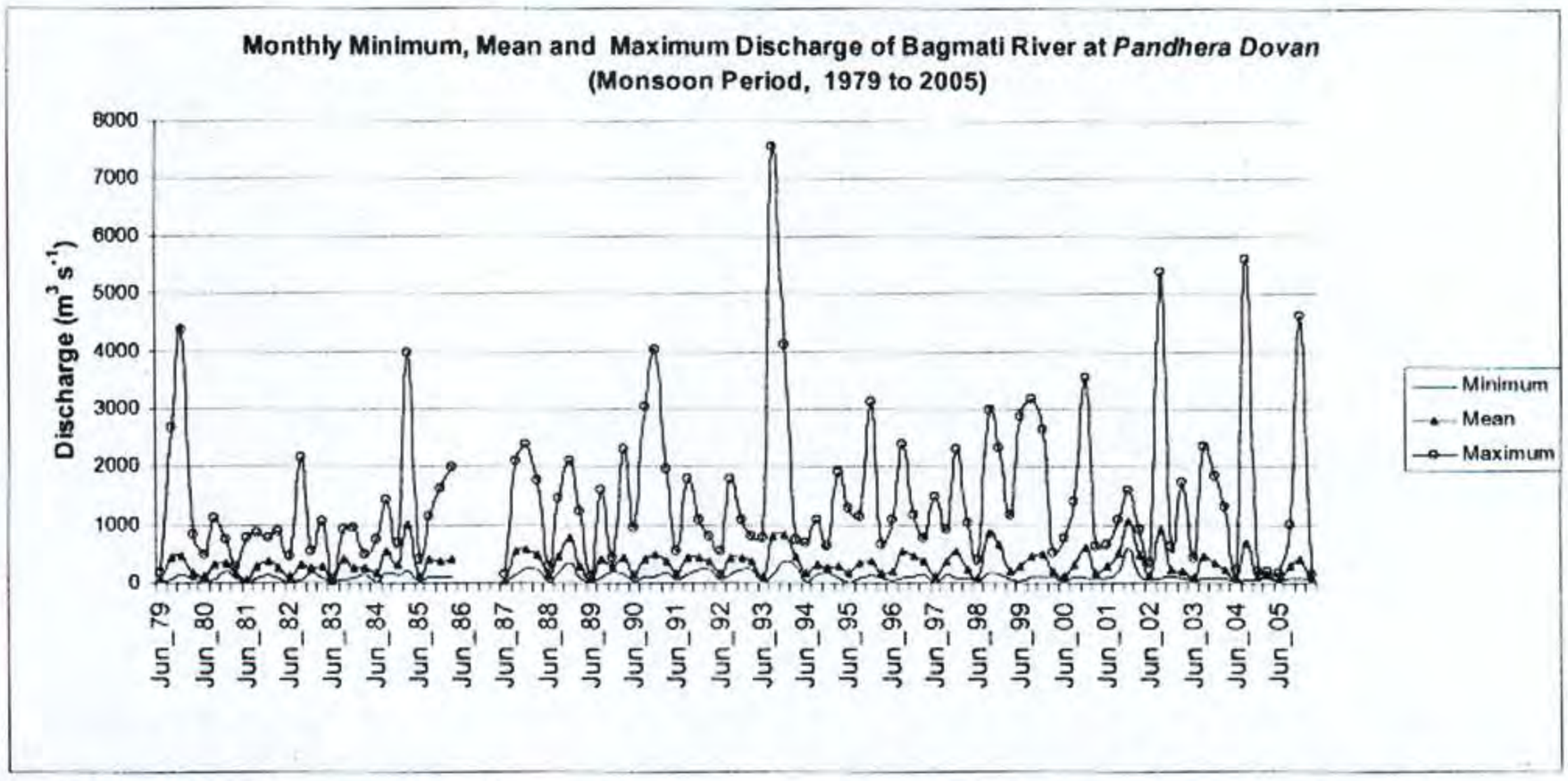

Figure 1: Hydrograph showing monthly minimum, mean and maximum discharge for the monsoon season (June to September) 1979 to 2005 measured at *Pandhera Dovan* of Bagmati River except 1986.

data was in ASCII format which can be easily transferred to Excel. The TRMM data was first assessed by comparing rain gauge data of the same period. Since there are 218 TRMM grids covering Nepal, only 5 grids were used for the comparison at this time. The selected 5 TRMM grids cover (Figure 2):

- the highest rainfall regime of Nepal, mountain topography (Lumle, grid No. 3).
- the lowest rainfall regime of Nepal, rain shadow, mountain topography (Jomsom, grid No. 4).
- Rain regime covering valley with highest number of rainfall stations (Kathmandu, grid No. 2).
- Rain regime mostly influenced by southeast monsoon, foot hills, and nearest to Bay of Bengal (Jhapa, grid No. 1).
- Rain regime relatively less influence by southeast monsoon and more influence by

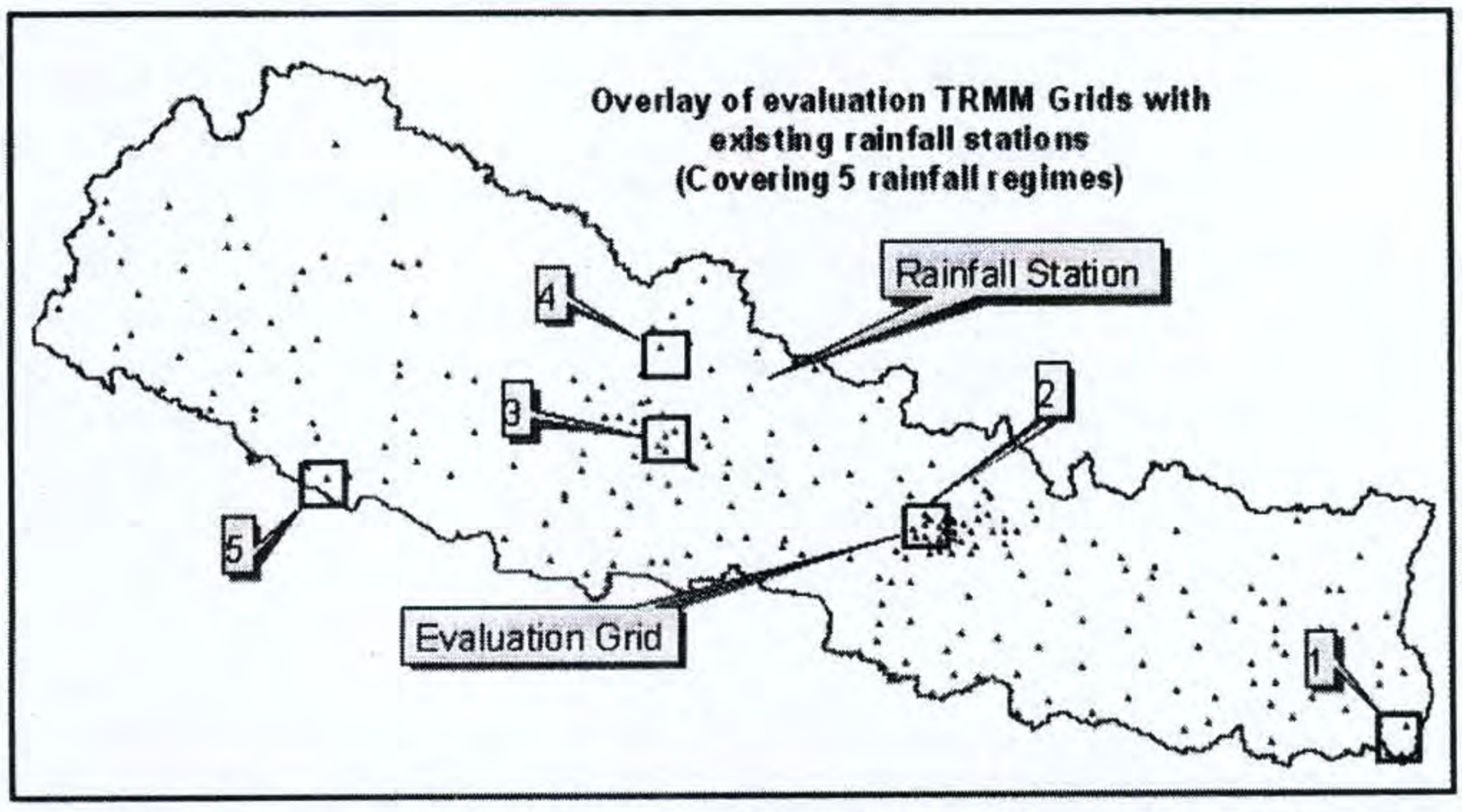

Figure 2: Rainfall station (2004) of Nepal and overlay of 5 TRMM grids to compare TRMM rain and observed rain. The grid boxes from east to west are Jhapa, Kathmandu, Lumle, Jomsom and Nepalgunj numbering 1 to 5 respectively representing five different rain regimes.

westerly disturbance, low land (Nepalgunj, grid No. 5).

Selected TRMM grids are taken as the representative samples of the five rainfall regimes of Nepal. Since the rain gauge networks are sparse, the number of rainfall station falling under the grids varies from one to nine (Figure 2). Central coordinates of TRMM grids with 0.25° x 0.25° dimensions are plotted in the country map with the boundary of Bagmati River basin (Figure 3).

Hourly rainfall data obtained from AWS of Budhanilkantha and Thankot station of Kathmandu valley were used to compare the diurnal variability of TRMM data. Both the AWS stations lie in the single TRMM grid of Kathmandu.

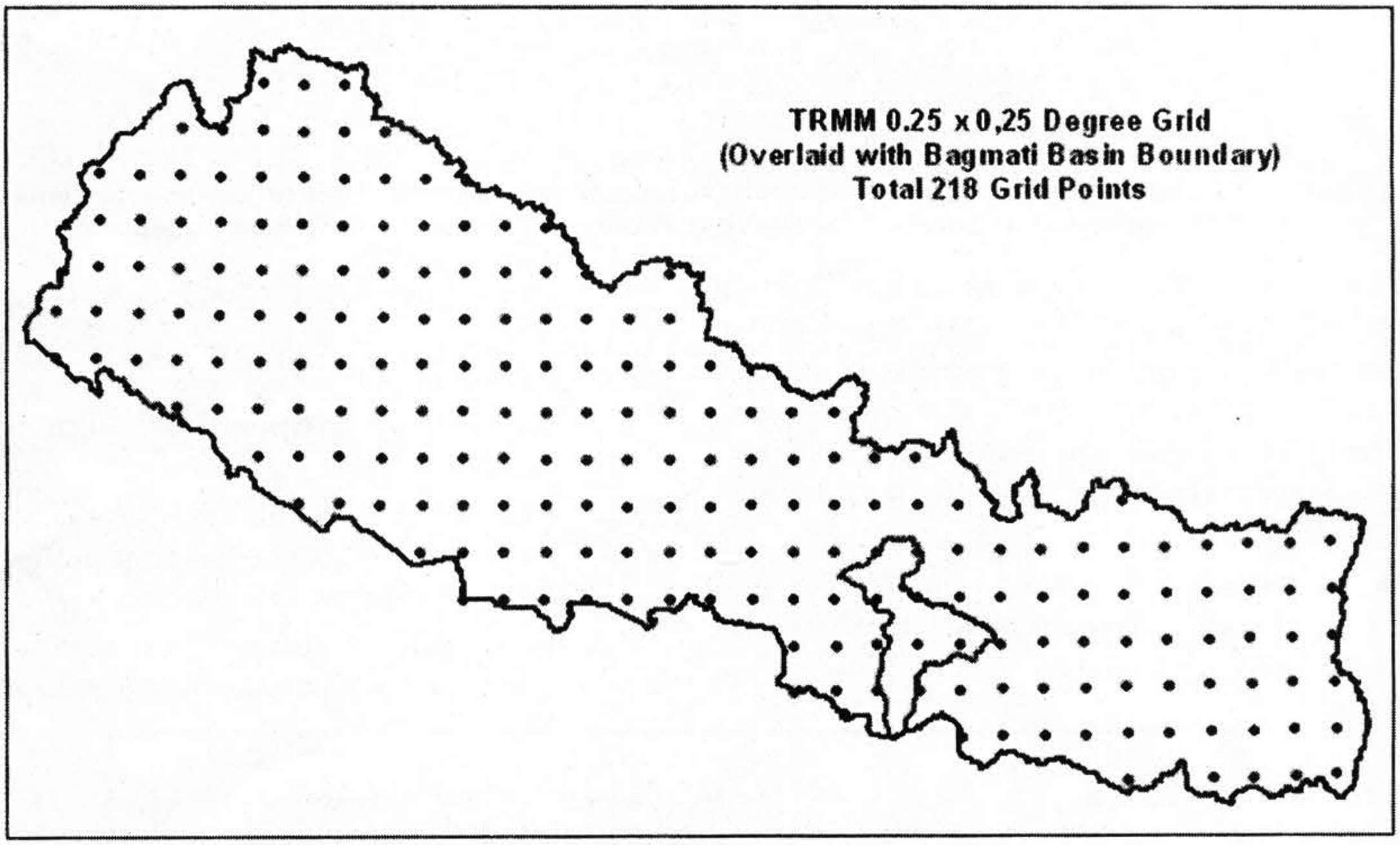

Figure 3: TRMM grids and Bagmati basin overlaid in the country map.

In this study different software packages were used. ArcView GIS 3.2 was used to make grid based comparison and various overlays, MS Excel was used for the data preparation and analysis, SPSS 10 was used regression analysis, and Fortran programming language was used for data handling and formatting.

3. RESULT AND DISCUSSION

3.1 GRID BASED COMPARISON OF TRMM AND OBSERVED RAINFALL

Five TRMM grids (as shown in Figure 2) are overlaid in the country map where rain gauge stations as well as annual rainfall are also plotted (Figure 4a and 4b). Figure 4a shows the rain gauge stations and corresponding annual rainfall for the year 2004 overlaid with two TRMM grids Lumle and Jomsom (highest and lowest rainfall regimes of Nepal within 50 km apart respectively). Lumle station has recorded 6096 mm rain in 2004. This grid [83.75° E lon and 28.25° N lat] has also covered 4 other rainfall stations names: Sallyan, Karki Net, Kushma and Sirkon which are also shown in Figure 4a.

Annual rainfalls of five rain gauge stations covered by Lumle grid varies from 1366 mm to 6096 mm in

2004. Within a single TRMM grid rainfall varies more than 5 times showing very high spatial variability. After simple averaging, the value come down to 3240 mm which is still higher than TRMM recorded value of 1875 mm in the same period. If there were more rainfall stations within the grid domain then the average value would be different.

Similarly, Jomsom grid [83.75° E lon and 28.75° N lat] has covered single rainfall station which is also shown in Figure 4a. TRMM estimated rain of the grid is 739 mm whereas observed rainfall is just 230 mm. If we see the lower edge of the grid (just outside the grid), rainfall exceeds more than 1100 mm. But no rain gauge stations are installed in this area. If we have more stations in this grid then the discrepancy between grid average and TRMM rain fields might be decreased. In case of Kathmandu grid [85.25° E lon and 27.75° N lat] 9 rainfall stations are within the grid domain (Figure 4b). Rainfall varies from 1105 mm to 2850 mm among the nine stations. When averaging, the value comes at 1639 mm whereas TRMM grid value for the same period (year 2004) is 1517 mm. It means when number of stations increased the TRMM rain and average of the observed rain tends to match. But there is still some variation if we go to monthly differential. Figure 5 shows monthly differences of TRMM rain and average of the observed rain. TRMM has underestimated the rain for the month of July for 3 grids (Lumle, Jhapa and Kathmandu) where it overestimated the rain for 2 grids (Jomsom and Nepalgunj). Similarly, TRMM has overestimated the rain in almost all months for the driest region, Jomsom grid (Figure 5a). In case of Kathmandu grid, maximum discrepancy of about 200 mm is seen for the month of July (Figure 5b). During the pre-monsoon period (April and May) TRMM has overestimated the rain for Kathmandu grid but TRMM has underestimated the rain for other grids (Figure 5a).

3.2 DIURNAL VARIABILITY OF HOURLY OBSERVED DATA AND THE TRMM DATA

Since temporal resolution of TRMM rainfall is 3 hours, it is possible to see the diurnal rainfall pattern. There is 8 set of rainfall data in 24 hours for a single grid. Here is this study, two TRMM grids, one of Kathmandu valley [85.25° E lon, 27.75° N lat] and another of south of Kathmandu [85.50° E lon, 27.50° N lat] are used to see the diurnal variability of rainfall. Total rainfall observation for a single grid in the year 2004 was 366 x 8 which is equal to 2928. Out of that very few values were

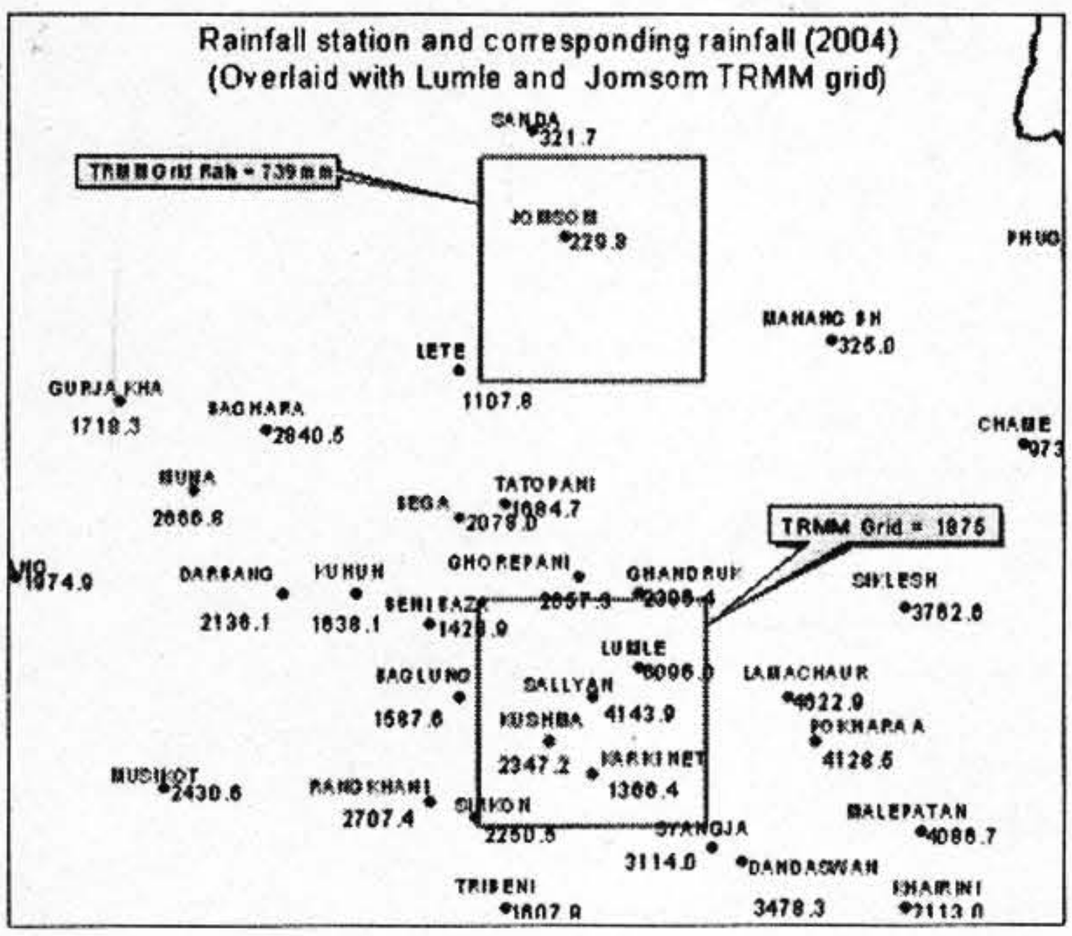

Figure 4: Rainfall station and corresponding rainfall for the year 2004 overlaid with a. Lumle and Jomsom grid b. Kathmandu grid.

missing due to satellite data transmission failure or other reasons. These data are grouped into 3-hourly basis. Diurnal variability of hourly rainfall data of 2-AWS stations (Budhanilkantha and Thankot) and two-TRMM grids are plotted in Figures 6a to 6d. Local time is plotted in X-axis and cumulative annual rainfall for that particular local time is plotted in Y-axis. TRMM Kathmandu grid (Figure 6a) has two maxima at 03:00 and 18:00 hours. The minimum occurs at 12:00 hours. There is gradual fall of rainfall between 03:00 to 12:00 hours. Rainfall increases sharply afterwards. Another TRMM grid south of Kathmandu (Figure 6b) has single prominent maximum at 00:00 hours (mid-night) and rainfall decreases sharply till the early in the morning. There is local maximum at 15:00 hours and rainfall further decreases to another local minimum at 18:00 hours. The AWS data of Budhanilkantha station has two prominent maxima at 01:00 hours and 22:00 hours (Figure 6c). Whereas in case of Thankot station single prominent maximum occurs at 03:00 hours and another local maximum is also observed at 17:00 hours, (Figure 6d).

In general, TRMM has well captured the diurnal variability of rainfall as compared to AWS data. Rainfall maximum has occurred at mid night and reach minimum in early in the morning. Rainfall increases gradually after noon and reach local maximum in the evening hours. Similar result was obtained by Barros et al. (2000) for low altitude (780 m) rainfall station, Khudi, of Nepal about 120 km west from Kathmandu (1350m) where heavier rain occurs at late night or early morning and reach minimum at late morning hours.

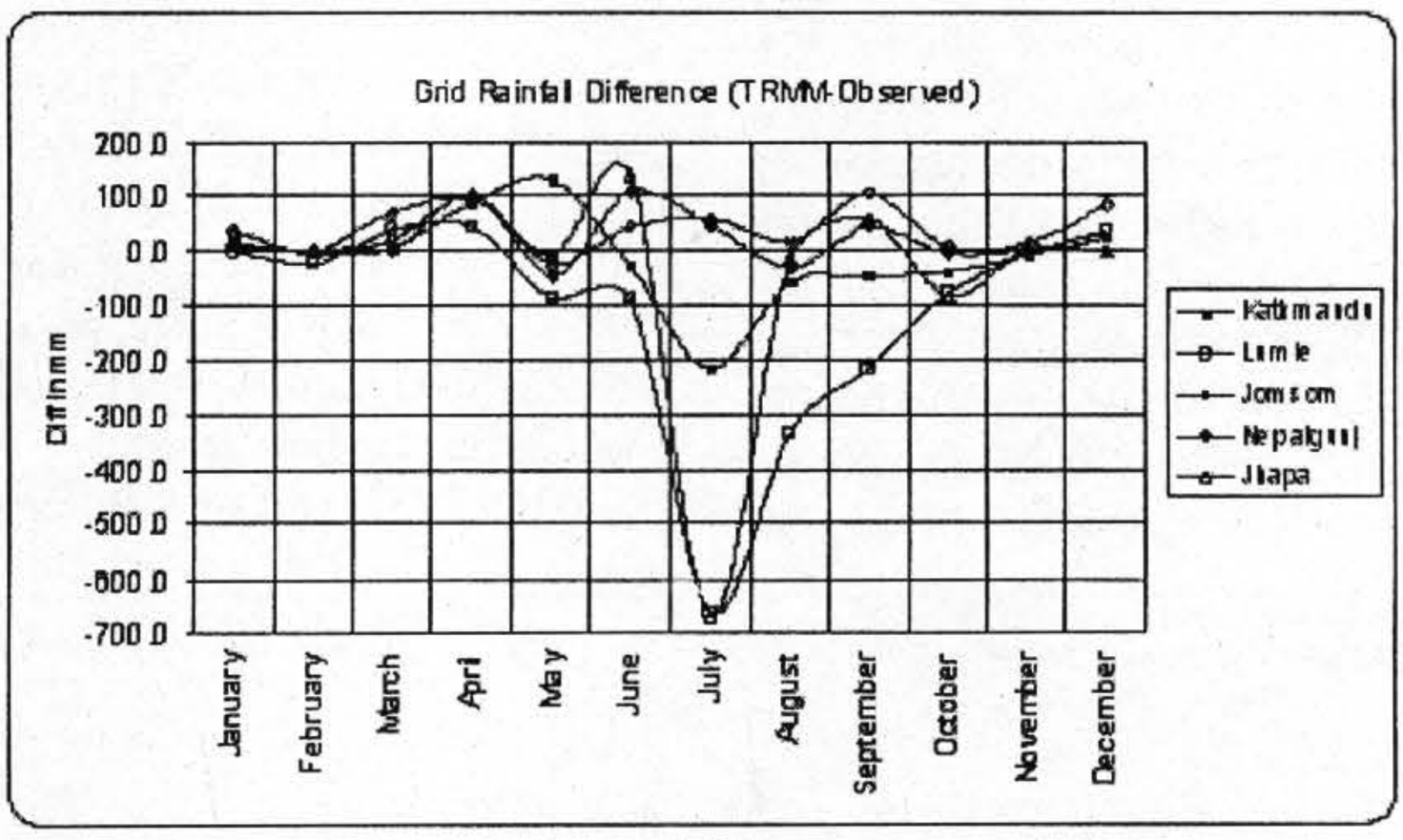

(a)

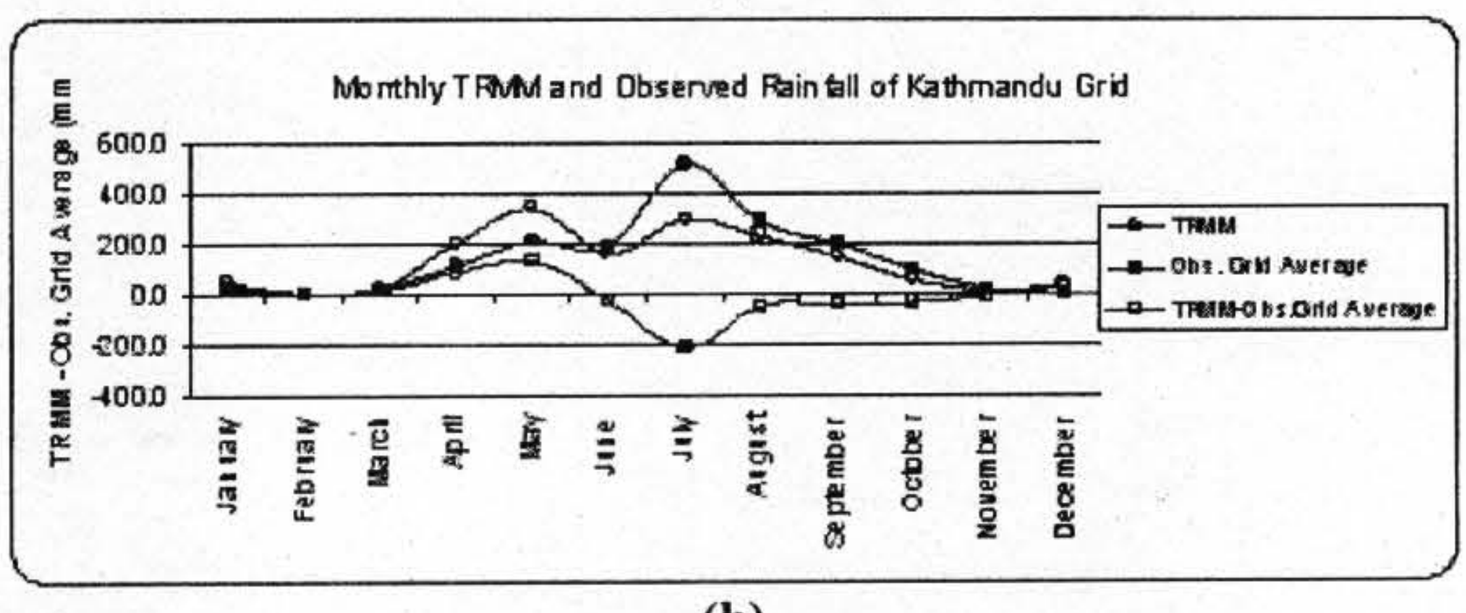

(b)

Figure 5: Differences between TRMM and observed rain within the grid domain for a. all five grids (above) and b. Kathmandu grid (below).

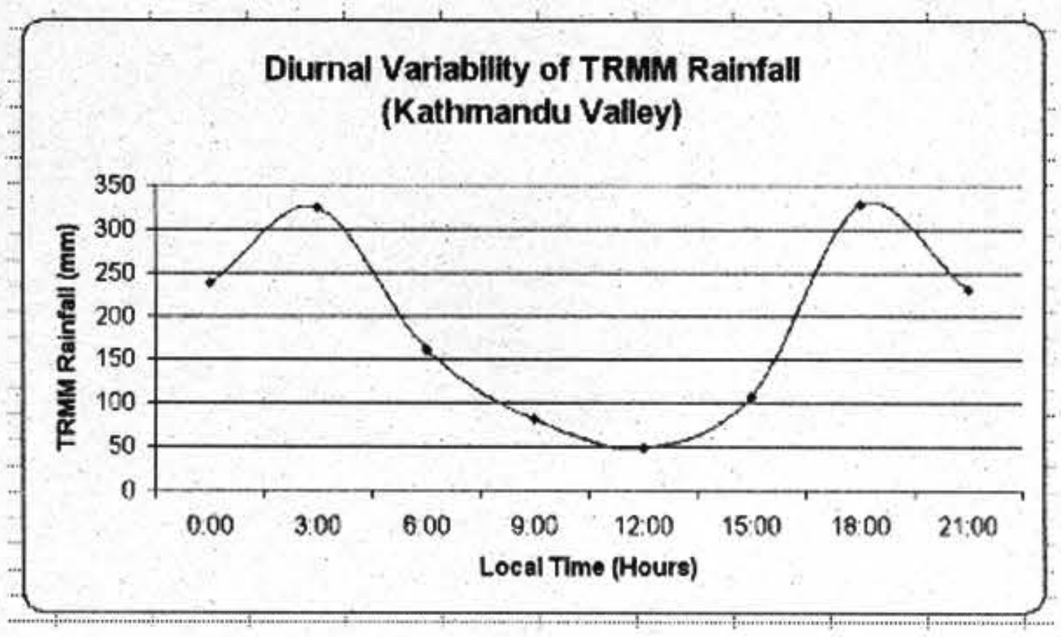

(a)

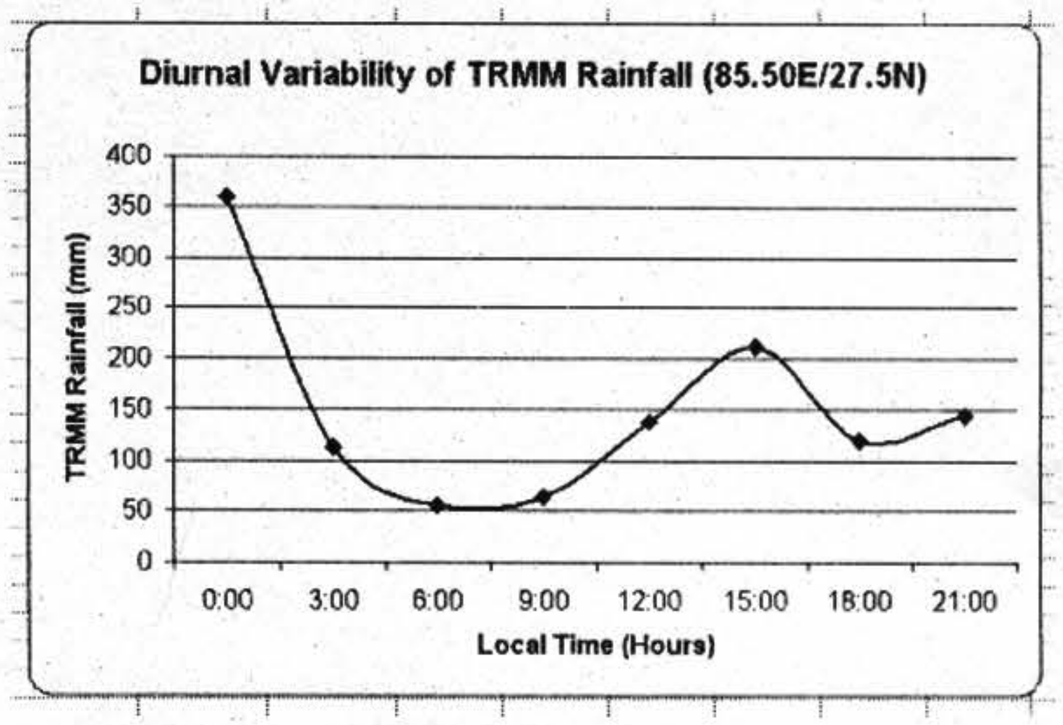

(b)

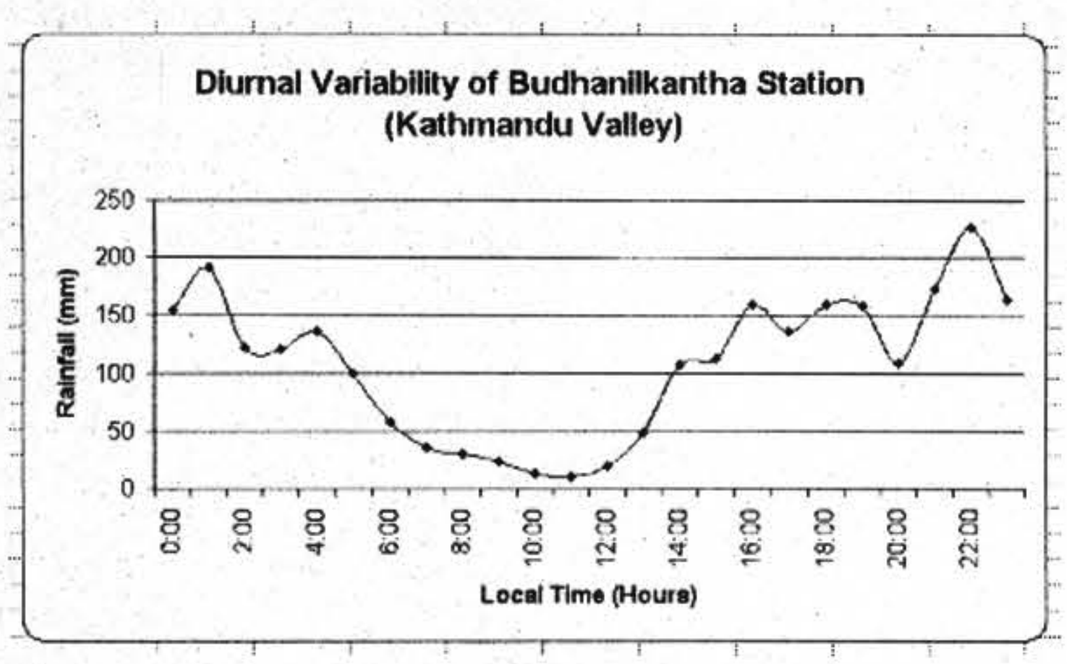

(c)

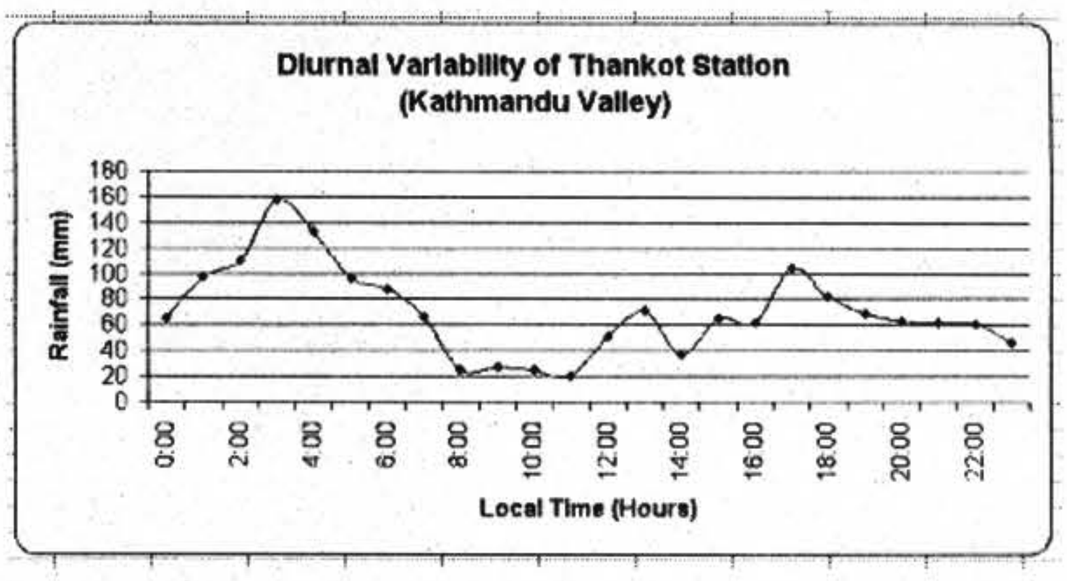

(d)

Figure 6 Diurnal Variability of (a) TRMM Kathmandu grid [85.25° E lon, 27.75° N lat] upper left, (b) TRMM grid [85.50° E lon, 27.50° N lat] south of Kathmandu valley upper right, (c) Budhanilkantha AWS station (85.36° E lon, 27.78° N lat) lower left, (d) Thankot AWS station (85.20° E lon, 27.68° N lat) lower right.

3.3 TIME SERIES AND SCATTER PLOTS OF OBSERVED RAIN AND TRMM RAIN

There were 19 rainfall stations and 11 TRMM grids (for numbering scheme see Figure 8a) in the basin up streams which can contribute to the discharge at *Pandhera Dovan* gauging site. Figure 7a shows the time series rainfall sum of TRMM grid (11 grids) and total observed rain (19 stations) for the monsoon period 2004. Figure 7a shows that most of the days TRMM has underestimated the rain. But the TRMM has captured the peak very well. Although it is not done here, a bias of the TRMM rain can be calculated by comparing with all Nepal rainfall station data for different rain regimes and months. So that TRMM rain can be adjusted accordingly.

Scatter plot of sum of 11 TRMM grids and sum 19 rainfall stations is shown in Figure 7b. The correlation between observed rain and TRMM rain is about 0.7, $R^2 = 0.48$ (Figure 7b). As we noticed, from the Figure 8a, that the basin does not fully cover all 11 grids. Some grids share very little area in the basin. In the next step each TRMM grids' rainfall are weighted according to areal contribution in the basin (see right side table of Figure 12). The scatter plot after applying the weighting factor in the TRMM grids is shown in Figure 8b where coefficient of determination has been increased by 16 per cent ($R^2 = 0.56$) as compared to Figure 7b.

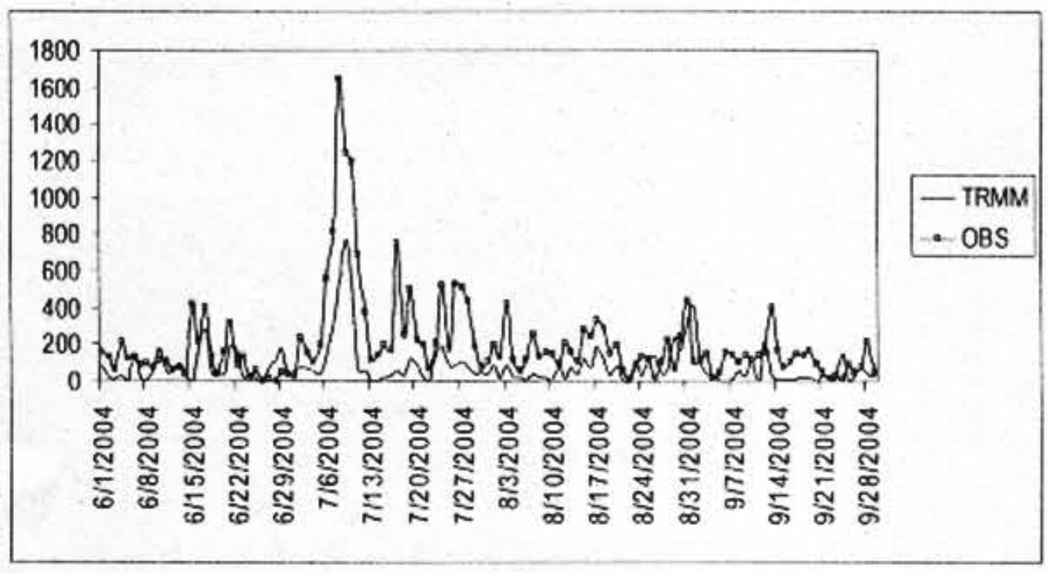

(a)

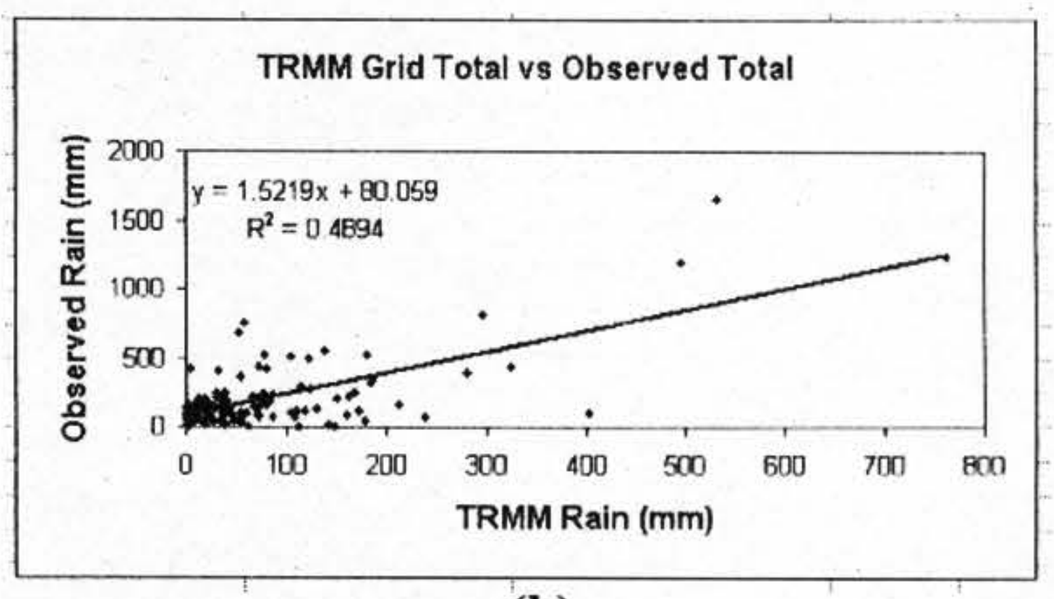

(b)

Figure 7: (a) Time series plot of daily total rainfall of all rain gauge station falling under the basin and the 11 TRMM grids total (partially and fully) under the same basin left, (b) scatter plot of the same data for the monsoon 2004, right.

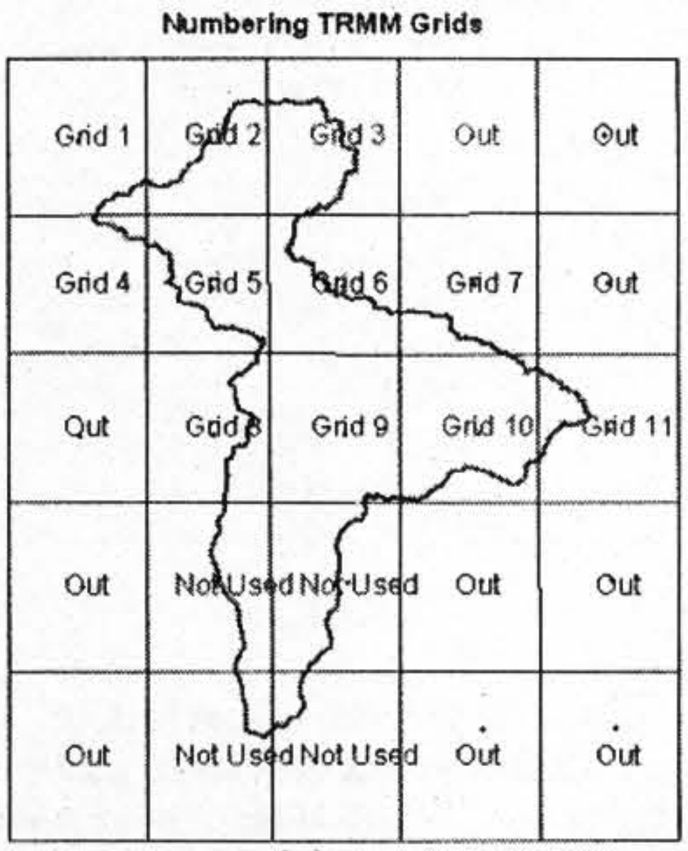

(a)

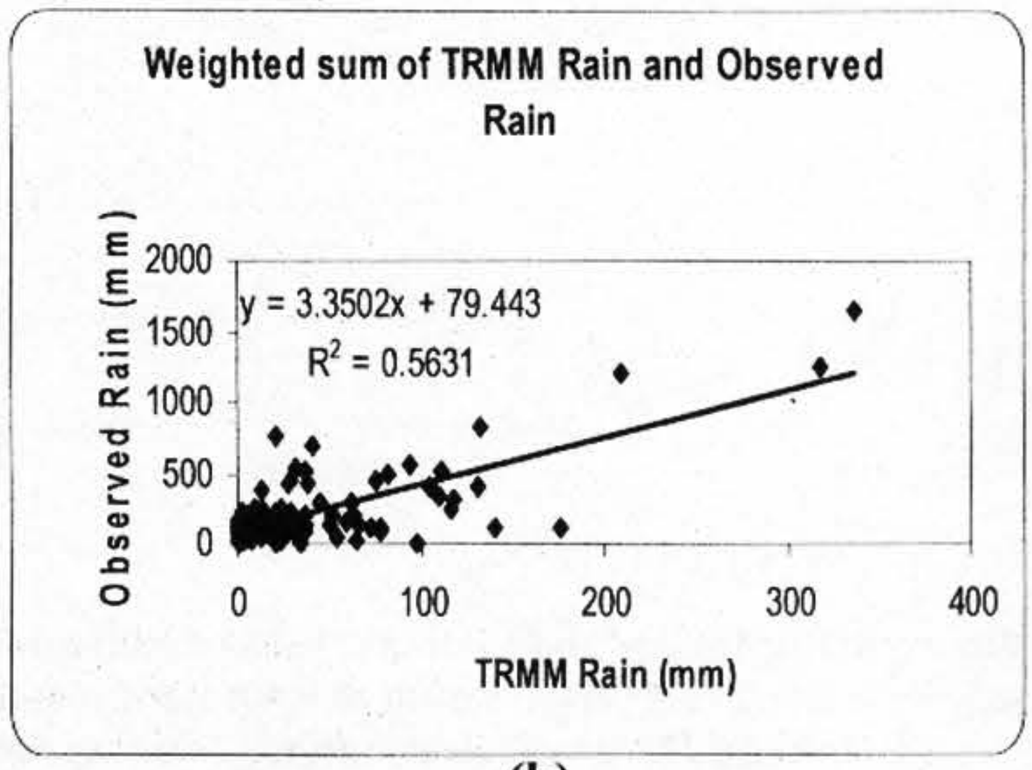

(b)

Figure 8: (a) Bagmati basin overlaid in the TRMM grid. (b) Scatter plot of weighted sum of TRMM grids and total observed rain for the monsoon period 2004.

3.4 FREQUENCY ANALYSIS OF 3-HOURLY TRMM RAIN FIELD

Since TRMM provides 3-hourly rain, it is possible to analyze the 3-hourly rainfall intensity throughout the monsoon period. During the monsoon period (June to September) total 976 (122 days x 8 times/ day) rainfall values for a single grid are available. For the frequency analysis, sum of all 11 grid's 3-hourly rainfall versus date and time are plotted in Figure 9. Not all the rainfall values are shown in Figure 9. Three-hourly grid sum rainfall (without applying weighting factor) is divided into four categories: >10mm, >20mm, >30mm and >40 mm. This information is particularly useful to flood routing. Once we know the input we can track the wave flow along the stream. But in this study, this analysis is not done due to unavailability of hourly discharge data. There are 123 events where rainfall occurs >10mm per 3-h which is about 13% of total population, 60 events with >20 mm, 42 events with >30 mm and 22 events with >40 mm (Figure 9a to 9d respectively). The highest 3-hourly TRMM rainfall intensity for this monsoon period was 157 mm.

3.5 RAINFALL RUNOFF RELATIONSHIP

Scatter plots of observed total rainfall and same day and next day discharge are plotted in Figure 10a and 10b respectively. There is higher correlation between the same day rainfall and same day discharge data as compared to day+1 discharge. The coefficient of determination is 0.68 for the same day data and 0.56 for the day+1 data. It can be

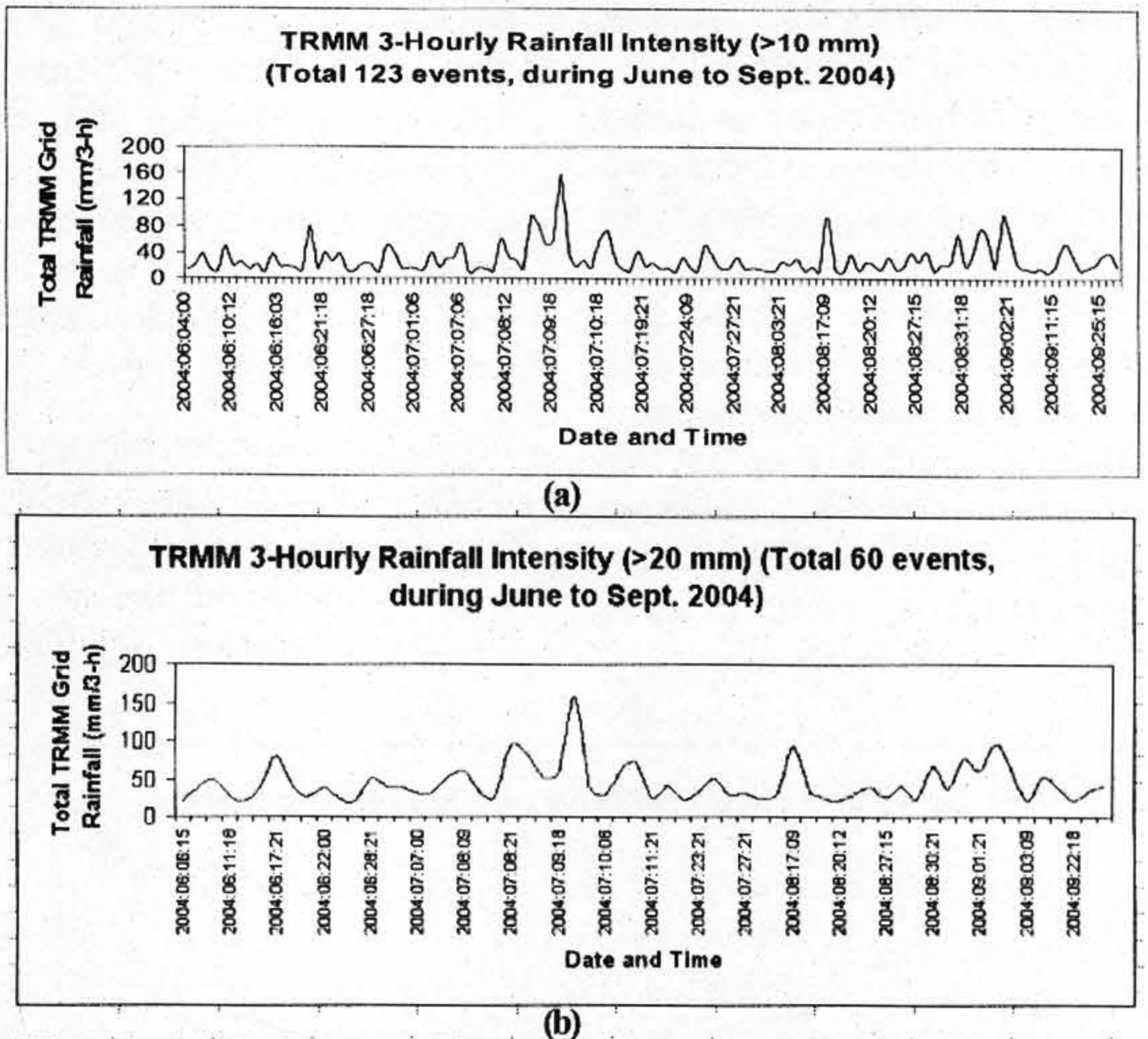

Figure 9: Three-hourly rainfall intensity of TRMM rain, plotted for different intensity level. (a) >10 mm, (b) >20 mm, (c) for >30 mm and (d) > 40 mm

firmly says that time of concentration at *Pandhera Dovan* station does not exceed 24 hours. Similarly, TRMM data is also plotted against the discharge data and the scatter plots are shown in the Figure 11. TRMM grid sum without applying weighting factor and applying with weighting factors are plotted in Figure 11 (a) and (b). It shows that weighted grid rainfall has better correlation with $R^2 = 0.60$ (Figure 11 b) with compared to non-weighted grid values $R^2 = 0.54$ (Figure 11a). TRMM is also plotted against the day+1 discharge and the scatter plot is shown in Figure 11c. Comparing the Figure 11 (a) and (c) we can again conclude that there is less correlation for day+1 discharge for the TRMM case also. If we apply some cutoff value of TRMM rain field to see the relationship between higher rainy events and discharge then the correlation is also increased noticeably. In case of those events with weighted grid rain field more than 50 mm per day, the R^2 goes up to 0.72 and similar case for more than 100 mm per day the value goes up to 0.75 (Figure 11 d & e).

In another scatter plot 3-hourly rain field of TRMM data is plotted against discharge data which is also highly correlated (correlation coefficient 0.8 (Figure 11f). It provides the basis to use high intensity 3-hourly data in rainfall-runoff estimation.

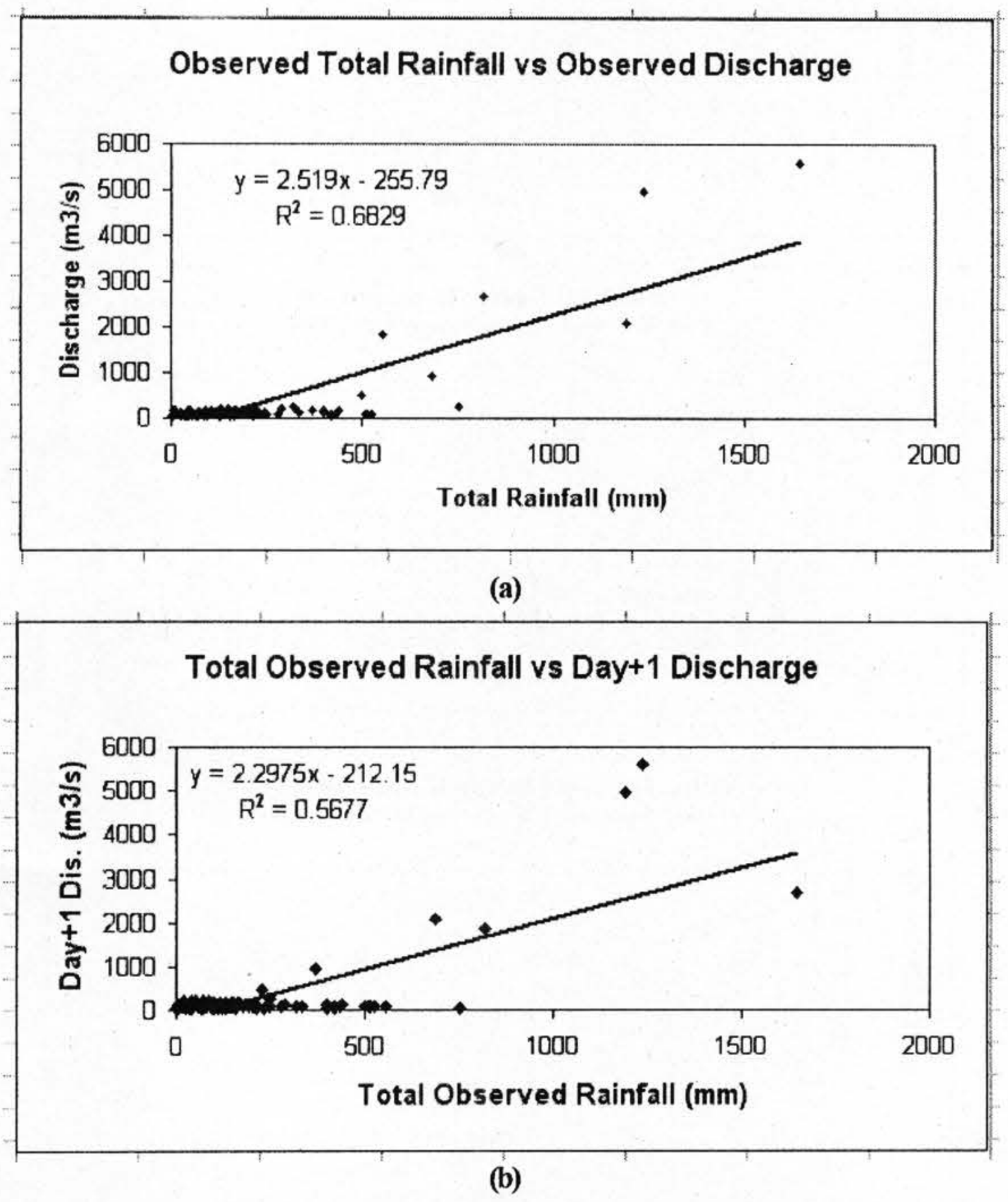

Figure 10: Scatter plots of (a) observed total rainfall and observed discharge for the same day (b) same as (a) but discharge is next day discharge (day+1).

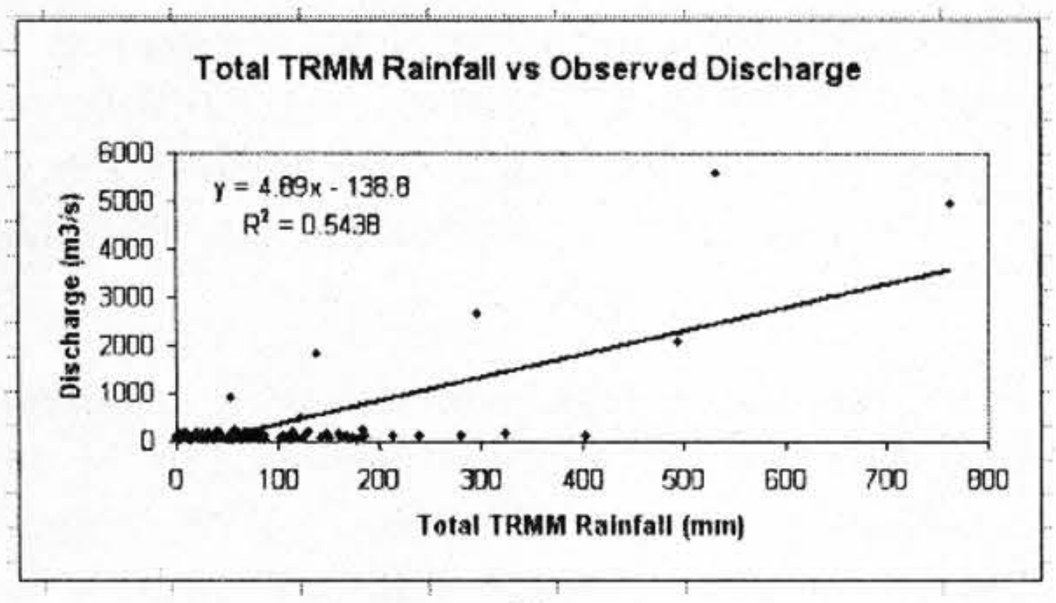

Figure 11: Scatter plots of (a) Total TRMM grid rainfall versus observed discharge data, upper left, (b) Weighted daily TRMM grid rainfall versus discharge, upper right, (c) Total TRMM rainfall versus next day discharge, middle left, (d). weighted TRMM rain >50 mm versus discharge, middle right, (e) weighted TRMM daily grid sum versus discharge, lower left, and (f) weighted 3-hourly grid sum > 100 mm versus discharge, lower right.

3.6 RAINFALL-RUNOFF MODELING

In this approach 3-hourly rain fields of TRMM are used to predict the discharge of the Bagmati River. First, data is prepared for regression analysis. Monsoon (2004) 3-hourly weighted grid rainfall and daily discharge data of the same period are used for the regression analysis. Regression coefficients thus obtained from the regression are used to predict the daily discharge of the monsoon (2005). As mentioned earlier, there are total 11 grids contributing runoff at river gauging station. These grids are aligned in three rows (same latitude) as shown in Figure 8a and Figure 12. Independent variables are 3-hourly rainfall and dependent variable is daily discharge. Following assumptions are taken into consideration:

- Maximum time of concentration is 24 hours
- Those grids lying in the same latitude have the same time of concentration.

- Discharge data used in this study is assumed to observe at 09:00 hours.

According to the first assumption, measured discharge, say, at 09:00 hours is a function of previous rainfall measured at 06:00, 03:00, 00:00, 21:00, 18:00, 15:00, 12:00, 09:00 hours of the previous day. If we consider all the grids as it is there will be 11 x 8 = 88 independent variables. To make model simpler, 11 grids are divided into three Blocks (Figure 12). Grids 1 to 3 (See also Figure 8 a) are in Block 1, grids 4 to 7 are in Block 2 and Grid 8 to 11 are in Block 3. After this the number of independent variable has been reduced to 24. The general regression equation can be written as:

$$Q(T) = f(B_{i(T-j)})$$

where $Q(T)$ is the discharge (dependent variable) at time T (multiple of 3-hour, say 09:00 hours), B_i is the block number varies from 1 to 3 and j is the previous 3-hourly time sequences varies from 1 to 8. Suppose if we want to estimate the discharge at 09:00 hours of June 10, then it is the function of Block1 rain measured at 06:00 hours, Block1 rain at 03:00 hours, ……., Block1 rain at 09:00 hours (June 9), Block2 rain at 06:00 hours, Block2 rain at 03:00 hours,……., Block2 rain at 09:00 hours (June 9), Block3 rain at 06:00 hours, Block3 rain 03:00 hours,……, Block3 rain at 09:00 hours (June 9).

Regression coefficients obtained from 122 observation data (monsoon 2004) using simple regression is shown in Table 1. Out of 24 independent variables 19 variables are significant within 0.01 level and 5 variables are not significant. Those variables representing less areal coverage and/or rainfall at minima are shown insignificant in the regression analysis.

To validate the regression model, daily discharge of 2005 monsoon period is predicted using the coefficients shown in Table 1. The adopted regression has well captured the daily peak of the monsoon 2005, although erratic fluctuation is also observed in those days where discharge is low (Figure 13 (a) and (b)). But there is still some room to improve the model which is discussed in the conclusion and recommendation section. The observed peak discharge of August 7, 2005 at *Pandhera Dovan* was 4600 $m^3 s^{-1}$ whereas predicted value is 4938 $m^3 s^{-1}$ which is 7% higher than the observed value. The correlation of the regression is 0.939 with standard error of estimate 285 $m^3 s^{-1}$ (Table 2). The erratic fluctuation especially in the low flow may be due to the inability to capture the actual rainfall by the TRMM, discharge data averaging rather than point specific discharge measurement. The general practice of discharge data measurement of the Bagmati River is that river level is observed 3 times a day at 09:00 hours, at 12:00 hours and at 18:00 hours. The daily average is simply the average of these three values. Discharge is estimated using rating curve updated frequently. But in this modeling, 09:00 hours is taken as the point of time of discharge measurement which also might be the cause of the erratic fluctuation.

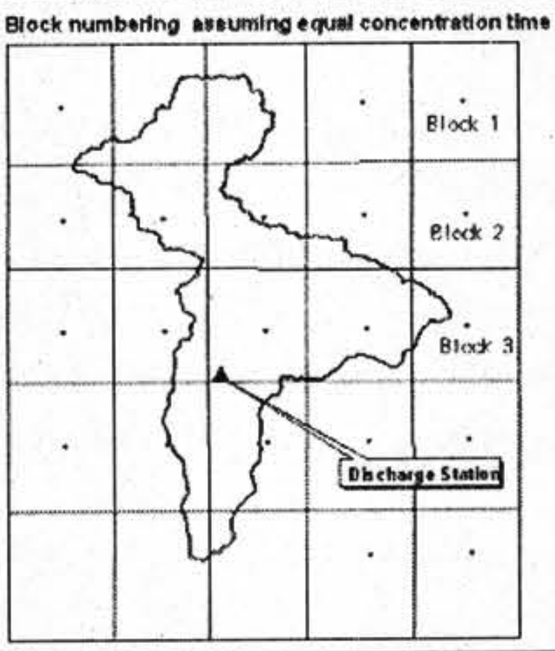

Grid Number	Weights
Grid 1	0.07
Grid 2	0.56
Grid 3	0.38
Grid 4	0.04
Grid 5	0.67
Grid 6	0.52
Grid 7	0.13
Grid 8	0.36
Grid 9	1
Grid 10	0.85
Grid 11	0.1

Figure 12: TRMM grids overlaid with the basin boundary and discharge station (left) and grid weights (table, right), for grid numbering scheme see Figure 8 (a).

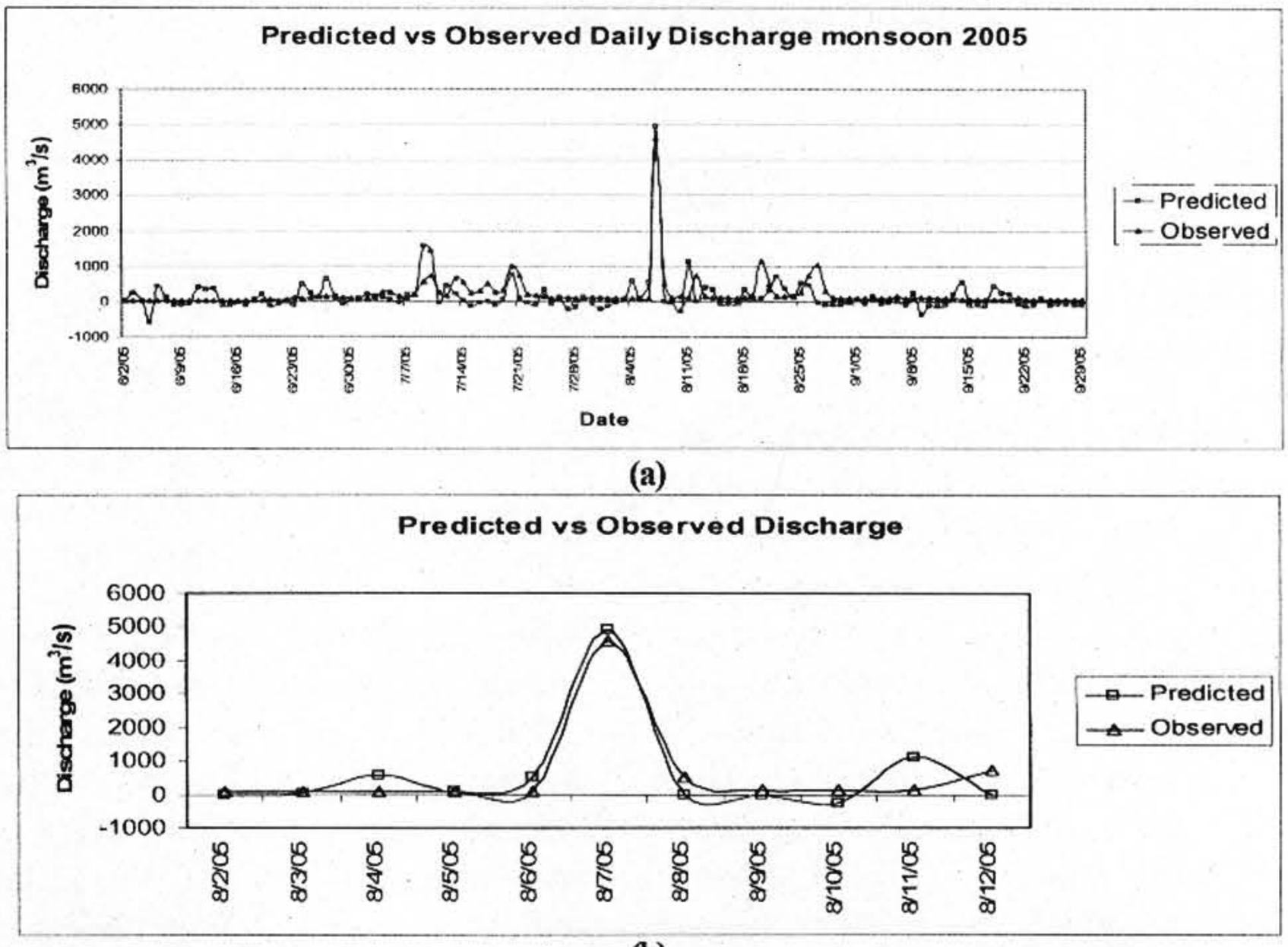

Figure 13: Predicted daily average discharge of Pandhera dovan of Bagmati River obtained from the regression analysis for (a) whole monsoon period from June to September 2005 and (b) a small window around the peak flow.

Table 1 Coefficients of Regression Analysis

Variable	Reg. Coeff.	Correlation Coe.	Correlation Status	Remarks
Discharge		1		Dependent Variable
Const.	-104.77			
$B_{1(T-1)}$	70.776	0.564	significant	
$B_{1(T-2)}$	-17.041	0.366	significant	
$B_{1(T-3)}$	-9.075	0.016	Not significant	Low areal coverage & rainfall minima
$B_{1(T-4)}$	14.319	-0.041	Not significant	Low areal coverage & rainfall minima
$B_{1(T-5)}$	17.887	-0.024	Not significant	Low areal coverage & rainfall minima
$B_{1(T-6)}$	-1.257	0.011	Not significant	Low areal coverage & rainfall minima
$B_{1(T-7)}$	-114.586	0.237	significant	
$B_{1(T-8)}$	138.705	0.613	significant	
$B_{2(T-1)}$	57.113	0.574	significant	
$B_{2(T-2)}$	28.899	0.649	significant	
$B_{2(T-3)}$	-27.334	0.264	significant	
$B_{2(T-4)}$	3.693	0.061	Not significant	rainfall minima
$B_{2(T-5)}$	18.495	0.117	Not significant	rainfall minima
$B_{2(T-6)}$	16.787	0.407	significant	
$B_{2(T-7)}$	-69.71	0.291	significant	
$B_{2(T-8)}$	36.946	0.669	significant	
$B_{3(T-1)}$	3.96	0.674	significant	
$B_{3(T-2)}$	-2.391	0.646	significant	
$B_{3(T-3)}$	17.984	0.413	significant	
$B_{3(T-4)}$	-1.629	0.292	significant	
$B_{3(T-5)}$	11.682	0.219	significant	
$B_{3(T-6)}$	0.165	0.268	significant	
$B_{3(T-7)}$	41.472	0.508	significant	
$B_{3(T-8)}$	36.954	0.706	significant	

Table 2: Model Summary of the regression

Model	R	R Square	Adjusted R Square	Std. error of the Estimate ($m^3 s^{-1}$)
1	0.939	0.881	0.851	284.96

4. CONCLUSION AND RECOMMENDATION

In this study, limited and sparse rain gauge data were used to asses the TRMM 3B42RT rainfields. Comparison was done on the grid basis. TRMM grid rainfall and observed rainfall falling under the grid domains were compared. It is found that TRMM rain fields are closely associated with areal average rainfall. Increase in number of stations falling under a grid domain decreased the differences between the TRMM rain and average of the observed rain. It was also found that TRMM has underestimated the rain for peak monsoon period for the wet rain regimes whereas it overestimated the rain for dry rain regimes.

Diurnal variability of rainfall was analyzed using hourly data of 2 AWS stations and 2 TRMM grids. TRMM has well captured the diurnal variability pattern as compared to AWS data. Various scatter plots of TRMM rain and observed rain, observed rain and discharge, TRMM rain and discharge with and without applying weighting factors were plotted to see the correlation. All the correlations were positive with correlation coefficient 0.7 and more. It provided the basis to use the TRMM rain in flood forecasting.

A simple regression technique was adopted to generate the regression coefficients using the near real-time 3-hourly TRMM (3B42RT) data and daily average discharge of the same period. The model was validated by predicting daily discharge of monsoon 2005. The predicted peak discharge of 2005 was 7 per cent higher than the measured value. The correlation between independent variables (TRMM rain) and dependent variable (daily discharge) was 0.939 with standard error of estimate 285 $m^3 s^{-1}$. The measured value of discharge on August 7, 2005 was 4,600 $m^3 s^{-1}$ whereas predicted value was 4,938 $m^3 s^{-1}$. Since peak discharge is the main concern for the floods, the adopted approach was able to capture the peak discharge with enough accuracy.

Predicted discharge particularly at low flow is fluctuating severely. There is still some room to rectify the model using hourly discharge data instead of daily average value. Please note that instantaneous peak flows are used for flood forecasting. As mentioned under Data and Methods in the paper, average daily maximum for a day in 1993 was 7500 $m^3 s^{-1}$ whereas the instantaneous maximum for the same day was 16,000 $m^3 s^{-1}$. The two discharges will produce completely different flooding scenarios. The 7500 $m^3 s^{-1}$ flood will be moderate and manageable whereas the one with 16,000 $m^3 s^{-1}$ will be catastrophic. Further down scaling using hourly discharge data may help to predict the instantaneous flow.

The model can be extended to other basins to see the model performance. In the next phase of the ongoing AIT-JAXA mini-project the model will be improved using hourly discharge data and hope that satellite based rainfall will be applicable for flood forecasting.

ACKNOWLEDGEMENT

We heartily thank to Japan Aerospace Exploration Agency (JAXA) for supporting the AIT-JAXA Mini-Project financially and technically. We also thank to Department of Hydrology and Meteorology of Nepal for providing hydro-meteorological data used in this research.

REFERENCES

Bagmati Report, 2005. Preparation of Water-Induced Hazard Maps of the Bagmati River Basin Volume 1 (Main Report), 2005, Department of Water Induced Disaster Prevention, Kathmandu, Nepal

Barros, A.P., M. Joshi, J. Putkonen, and D.W. Burbank, 2000. A study of the 1999 monsoon rainfall in a mountainous region if central Nepal using TRMM products and rain gauge observation. Geophysical Research Letter, vol. 27, No 22 3683-3686.

Barros, A.P., 2004. On the Space-Time Pattern of Precipitation in the Himalayan Range: A Synthesis. GAME CD ROM Publication No. 11, T8APB19Oct04100318.

Boi, P., M. Marrocu, and A. Giachetti, 2004. Rainfall Estimation from infrared data Using an improved version of the Auto-Estimator Technique. International Journal of Remote Sensing, vol. 25, No. 21, 4657-4673.

Brown, John E.M. 2006. An Analysis of the performance of hybrid infrared and microwave satellite precipitation algorithms over India and adjacent regions, Remote Sensing of Environment 101 (2006) 63-81.

Delgado,German, Angel Redano, Jeronimo Lorente, Adolfo Magaldi, Marcus Jorge Bottino, Luiz Augusto Toledo Machado, 2006. Rainfall estimation over south America using the Precipitation RADAR product of the TRMM satellite, IR-VIS cloud classification and properties of convective systems, Proceeding of ERAD 2006.

DHM, 2007. Hydrological Database of Nepal, Department of Hydrology and Meteorology, Kathmandu, Nepal

Gorenburg, Ida Primus, Dennis McLaughlin, Dara Entekhabi, 2001. Advances in Water Resources 24 (2001) 941-953

Itou, Hisakazu and Kazuo Kera, 2006. Global Flood Alert System (GFAS), International Flood Network (IFNet) Secretariat, Infrastructure Development Institute Japan.

Kidder, Stanley Q., and Thomas H. Vander Haar, 1995. Satellite Meteorology An Introduction, Academic Press, San Diego, California

Levizzani, V., R. Amorati and F. Meneguzzo, 2002. A Review of Satellite-based Rainfall Estimation Methods, MUSIC (Multiple-Sensor Precipitation Measurements, Integration, Calibration and Flood Forecasting), European Research Project Report under the EVK1-CT-2000-0005.

Petty, Grant W., 1995. The status of satellite-based rainfall estimation over land. Remote Sensing and Environment, 51:125-137, Elsever Science Inc.

Sorooshian S., X. Gao, K. Hsu, R.A. Maddox, Y. Hong, H.V. Gupta and B. Imam, 2002. Diurnal Variability of Tropical Rainfall retrieved from combined GOES and TRMM Satellite Information, Journal of Climate, pp. 983–1001, American Meteorological Society.

Todd, Martin C., Chris Kidd, Dominic Kniveton, Tim J. Bellerby, 2001. A combined satellite infrared and passive microwave techniques for estimation of small-scale rainfall. Journal of Atmospheric and Oceanic Technology, American Meteorological Society, vol. 18, 742-755.

Xie, Pingping and Philip A. Arkin, 1996. Analysis of global monthly precipitation using gauge observations, satellite estimates, and numerical model predictions. Journal of Climate, vol. 9, 840-858